P15.3 AN EVALUATION OF MESOSCALE MODEL SIMULATIONS OF AN OSCILLATING DRYLINE

Mark R. Conder* and Richard E. Peterson
Department of Geosciences, Texas Tech University, Lubbock, Texas

1. INTRODUCTION

One of the many interesting forecasting "problems" facing the operational meteorologist is determining the evolution of the high plains dryline. Forecasts of the afternoon dryline position are frequently critical to the success of a convective initiation forecast. Numerous previous studies have already established the dryline's role of providing a near-surface boundary, enhancing the lift and convergence necessary for the development of thunderstorms. The quiescent dryline may be described as one that where the influence from a translating synoptic scale system is absent (Schaefer, 1986). Although the synoptically quiescent dryline does not generate as much severe convection as its dynamically-forced cousin, it is not uncommon to see isolated severe weather associated with it. As the horizontal resolutions of operational models increase (e.g. NCEP ETA from 22 to 12 km in 2001), forecasts of the dryline are becoming increasingly accurate. The quiescent dryline exists in a synoptic environment characterized by weak (but still meeting some minimum requirements) flow. This implies that the model PBL schemes will have paramount effects on the dryline forecast. For example, the daytime eastward motion of the dryline is accomplished through vertical turbulent mixing of the PBL (Hane, 2003). Previous model studies have shown that topography and soil moisture gradients are two very important controls that can affect the evolution of this process (e.g. Grasso et al., 2001). For this study, simulations were conducted of an oscillating southern plains dryline from 14-18 April 2002. Minimal thunderstorm activity occurred during this episode, so that storm-scale feedback to the environment was minimized. Two mesoscale models were employed, the PSU-NCAR MM5 and the CSU-ATMET RAMS. Near-surface in-situ measurements of the observed dryline are provided by 30 stations of the West Texas Mesonet. A comparison of model output to the observations is performed through a spatial analysis of dryline position and the calculation of mean bias and rmse of the water vapor mixing ratio.

2. THE DRYLINE OF 14-18 APRIL 2001

The evolution of synoptic-scale features associated with this dryline episode is fairly typical of early-season patterns. A fast-moving shortwave moved through the central U.S. on 13-14 and had sent a shallow cold front into the region.

* Mark R. Conder, Texas Tech University, Department of Geosciences, Lubbock, TX 79409-2101; email: mark.conder@ttu.edu

As southwesterly 500 hPa flow became established across the west-central U.S., a low level lee-side trough and southerly jet at 850 hPa developed. This enabled low-level moisture to be drawn northward from the Gulf of Mexico, first across south and central Texas and then up onto the Caprock. Finally, by the 19th, another shallow cold front dropped into the region, scouring out the deeper moisture. Figure 2 shows an overview of the synoptic features. The surface dryline oscillated across the domain during the period. In general the dryline began to move eastward in the morning, stalling during the late afternoon and early evening, and then reversing during the night. However, each oscillation of the dryline exhibited differences in speed, timing, direction, and distance traveled before stalling. Figure 3 depicts the evolution of the dryline. The motion of the dryline can also be readily seen via a time series of wind and dewpoint shown in Figure 4.

2. MODEL SIMULATIONS

Both the MM5 and RAMS models are generally classified as three-dimensional, non-hydrostatic primitive equation models. They can be configured with a wide variety of options and resolution depending on the phenomena undergoing investigation. Both have been successfully used with mesoscale resolution to simulate drylines in several investigations. For this study, the model runs were configured to be as similar as possible. Table 1 shows some of the configuration model details for the study.

Table 1: Short list of configuration options used in the model simulations.

Parameter	Specification
Number of grids	2
Grid resolution	18 km (grid 1), 6 km (grid 2)
Dimensions	47 by 47 (grid 1 and 2)
Grid center point	24.0 lat, -101.7 lon
Initialization	NCEP ETA model initialization (40 km AWIPS Grid 212)
Simulation duration	60 hours
Output	Lowest sigma-levels every hour
Lateral boundary nudging	NCEP ETA model every 12 hours
PBL Scheme	MM5: MRF (1st order closure) RAMS: Mello-Yamada TKE K
Elevation data	USGS 30-sec (inner grid)
Land use data	USGS 1-km

The model domains were configured with two considerations in mind. Foremost was the horizontal resolution required to accurately model the dryline. A 6-km grid spacing (inner grid) was chosen. Typically, between four and six grid points are required to resolve a meteorological feature. Thus, a 6-km grid can resolve features approximately 24 to 36 km or greater in horizontal dimension. Secondly, for verification, the model output was to be compared with an OA grid created from observations from the surface network. The ~20 km average spacing of the West Texas Mesonet compares favorably to the model resolution. The model domains are shown in Figure 1.

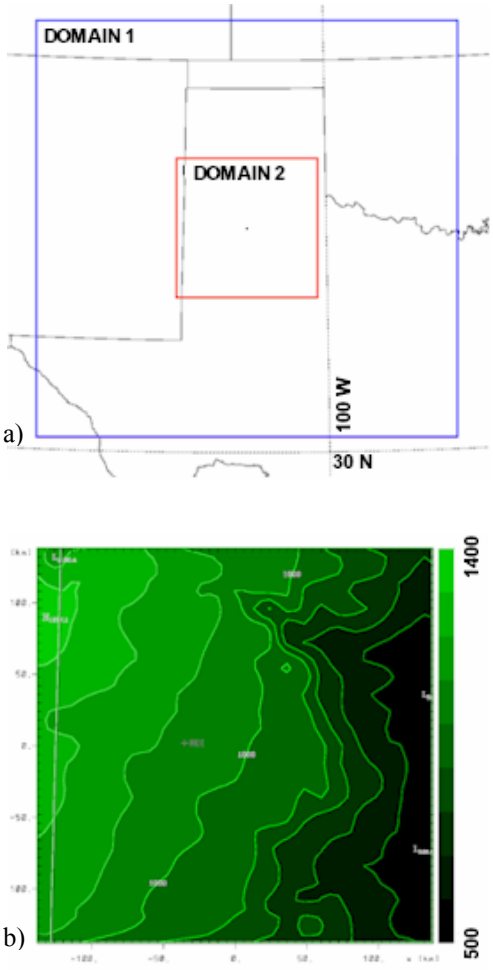

Figure 1. a) Domains of the MM5 and RAMS model configuration showing the coarse and nested grids. The domains are centered near the Reese Center West Texas Mesonet station. b) The topography of the inner grid is contoured and shaded every 100 meters. The Caprock Escarpment is approximately located along the 900 meter contour and the large valley on the north side of the inner grid is Palo Duro canyon.

3. ANALYSIS OF MODEL RESULTS

Figures 5 and 6 respectively depict the modeled dryline for the MM5 and RAMS simulations. First of all, the simulations show that the simulations do create a moisture gradient along with a wind shift that is similar to observed dryline behavior. These figures also show that the accuracy of the location of the 8.5 g kg^{-1} contour generally decreases with each iteration, particularly in the case of the RAMS model. While both models depict the diurnal oscillation on the 15-16th, the MM5 begins with the dryline located too far east (figure 5a), while the RAMS initial location is more accurate. The MM5 also retreats the dryline too early in the evening. The RAMS timing is better, however it begins to diverge from the observed dryline by greatly underestimating the extent of the westward retreat (figures 3b and 6b). During the day of the 16th, both models advance the dryline too quickly eastward (figures 5c and 6c). The MM5 begins the dryline's retreat several hours too early, but is roughly accurate with the dryline's position by the morning of the 17th (Figure 5d). The RAMS simulation however, does not retreat the dryline back into the experimental domain. A plot of the mixing ratio trace from the Reese Site (approximate center of the domain) shown in Figure 4 can be compared to the model forecasts. Figure 7a shows that the MM5 forecast looks similar in a broad sense. However, one can notice that in general the change in mixing ratio occurs much quicker in the observed data. The RAMS forecast falters fairly quickly, underestimating even the first moisture return. By examining the model forecasts of the u-component of the 10 meter wind in figure 8, one reason for the RAMS failure to forecast the westward motion of the retreating dryline is due to the lack of an easterly component to the forecast wind.

4. ACKNOWLDGEMENTS

The authors wish to thank the Wes Burgett of the West Texas Mesonet for providing the surface data. The authors also thank Tim Doggett, Air Worldwide Corp., and David Ovens, Univ. of Wash., for their assistance with converting the model output to GEMPAK format.

This research was funded in part by the U.S. Army Department of Defense contract #DAAD-13-00C-0048.

5. REFERENCES

Grasso, Lewis D., 2000: A numerical simulation of dryline sensitivity to soil moisture. *Mon. Wea. Rev.,* **128**, 2816-2834.

Hane, Carl E., 2004: Quiescent and synoptically-active drylines: A comparison based upon case studies. *Meteor. Atmos. Physics.,***86-3**,195-211.

Schaefer, Joseph T., 1986: The dryline. *In Mesoscale meteorology and forecasting* (Ray, P. S., ed), American Meteorological Society, Boston, MA, pp 549-572.

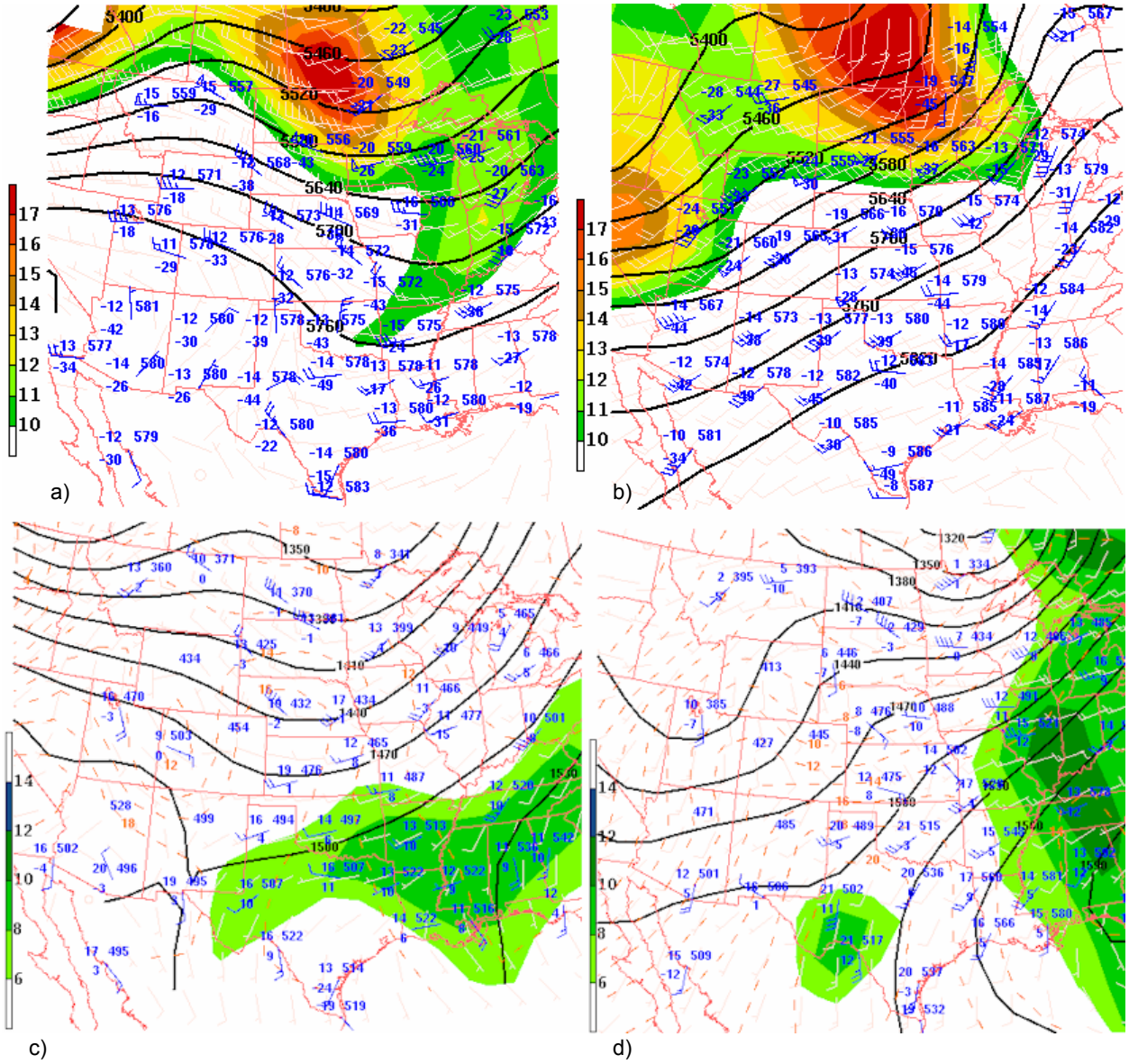

Figure 2. Objectively analyzed constant pressure maps for a) 04-14-2002 12 GMT at 500 hPa, b) 04-14-2002 12 GMT at 850 hPa, c) 04-17-2002 12 GMT at 500 hPa, and d) 04-14-2002 12 GMT at 850 hPa. 500 hPa geopotential heights are contoured every 40 meters. 850 hPa heights are contoured every 30 meters. Station plot depicts the wind in knots, temperature and dewpoint in degrees Celsius, the 500 hPa heights in decameters and the 850 hPa heights in meters minus 1000. Units of absolute vorticity shading on the 500 hPa maps are $10^{-5}s^{-1}$. Dewpoints greater than 6 degrees Celsius are shaded on the 850 hPa maps.

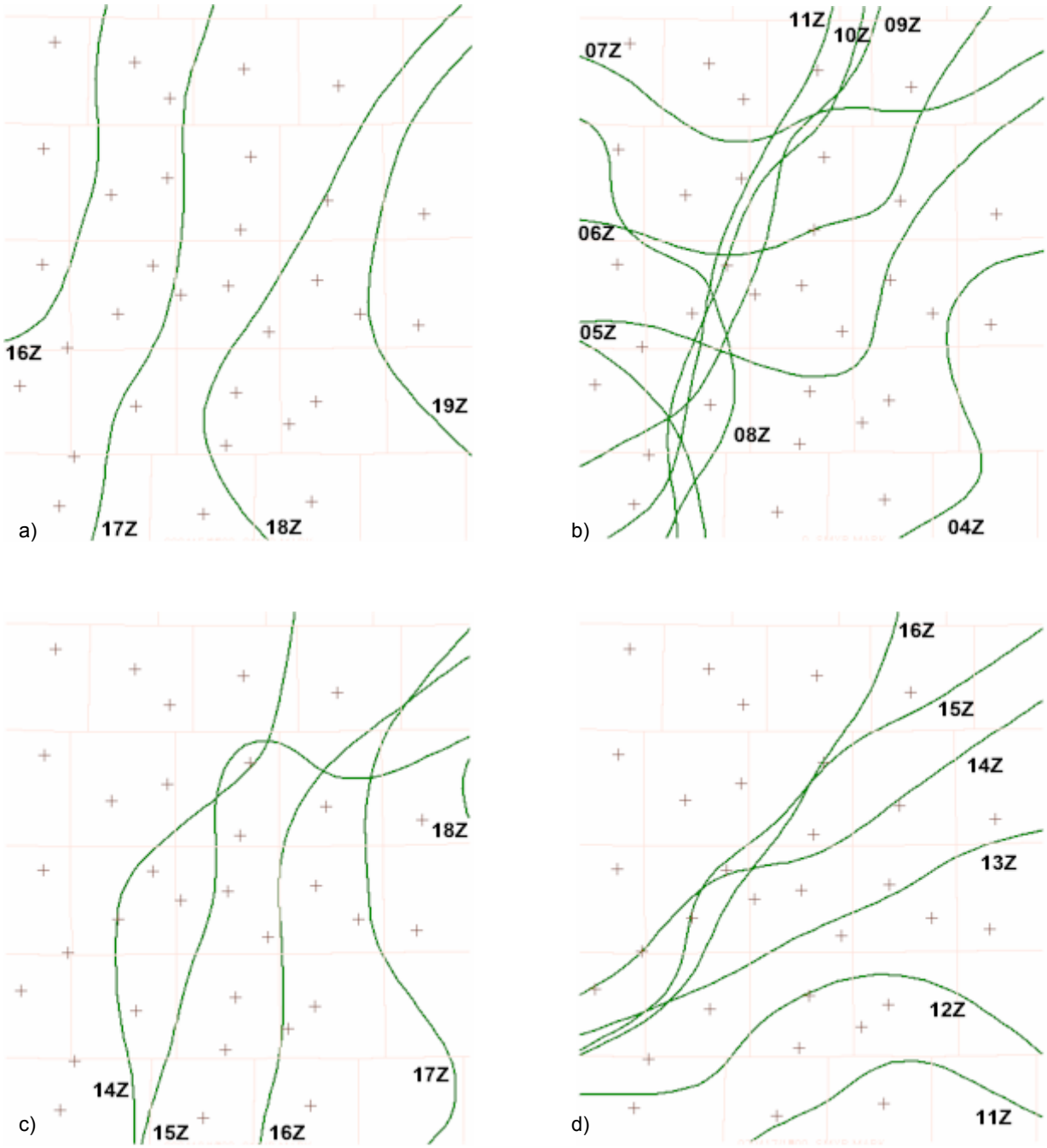

Figure 3. Plots of the 8.5 gkg^{-1} mixing ratio contour for the oscillating dryline. a) 16 – 19 GMT 15 April, b). 04 – 11 GMT 16 April, c) 14 – 18 GMT 16 April, and d) 11 – 16Z 17 April.

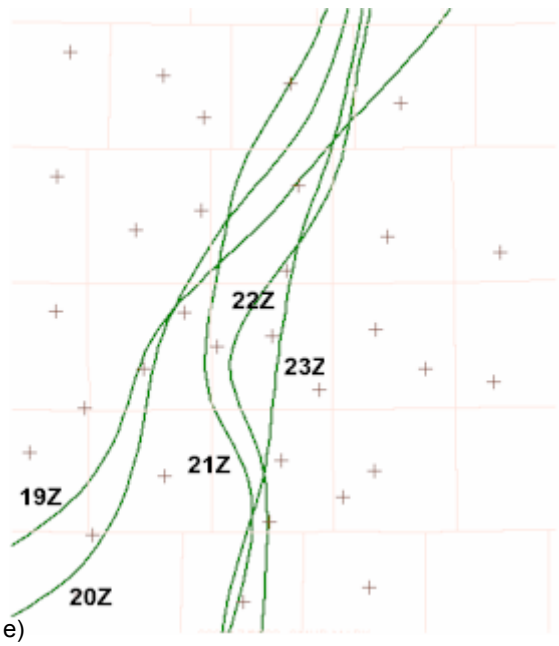

e)

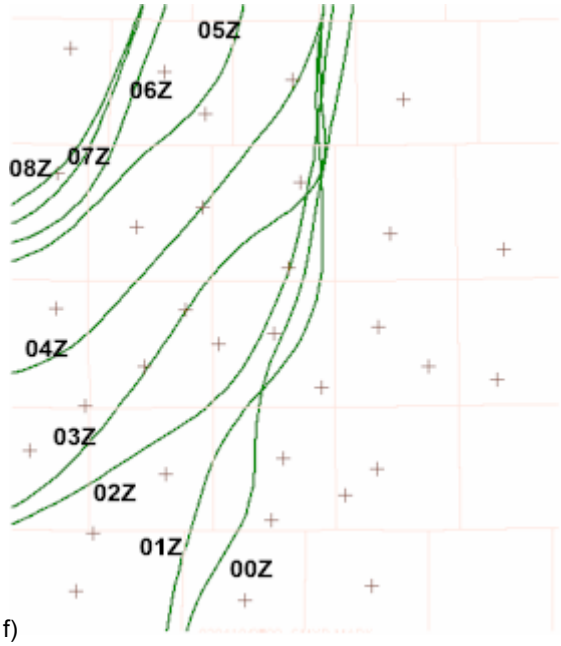

f)

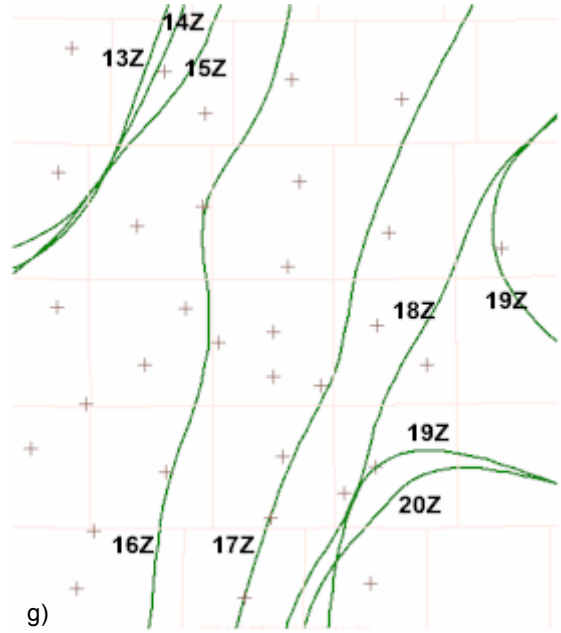

g)

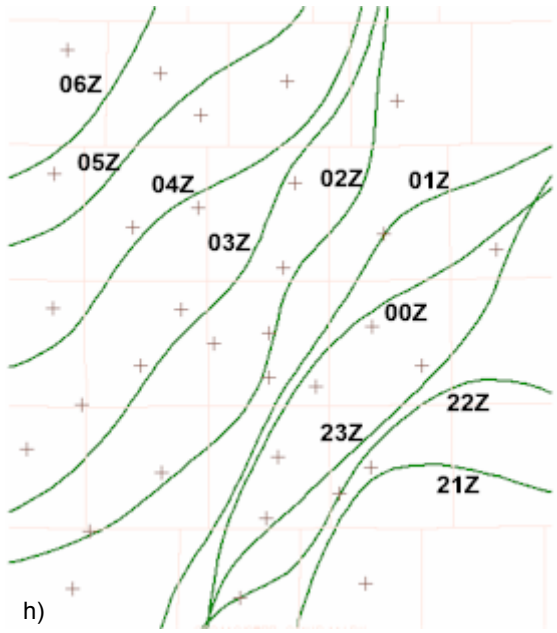

h)

Figure 3 continued. Plots of the 8.5 gkg^{-1} mixing ratio contour for the oscillating dryline. e) 19 – 23 GMT 17 April, f). 00 – 08 GMT 18 April, g) 13 – 20 GMT 18 April, and h) 21 GMT 18 April – 06Z 19 April.

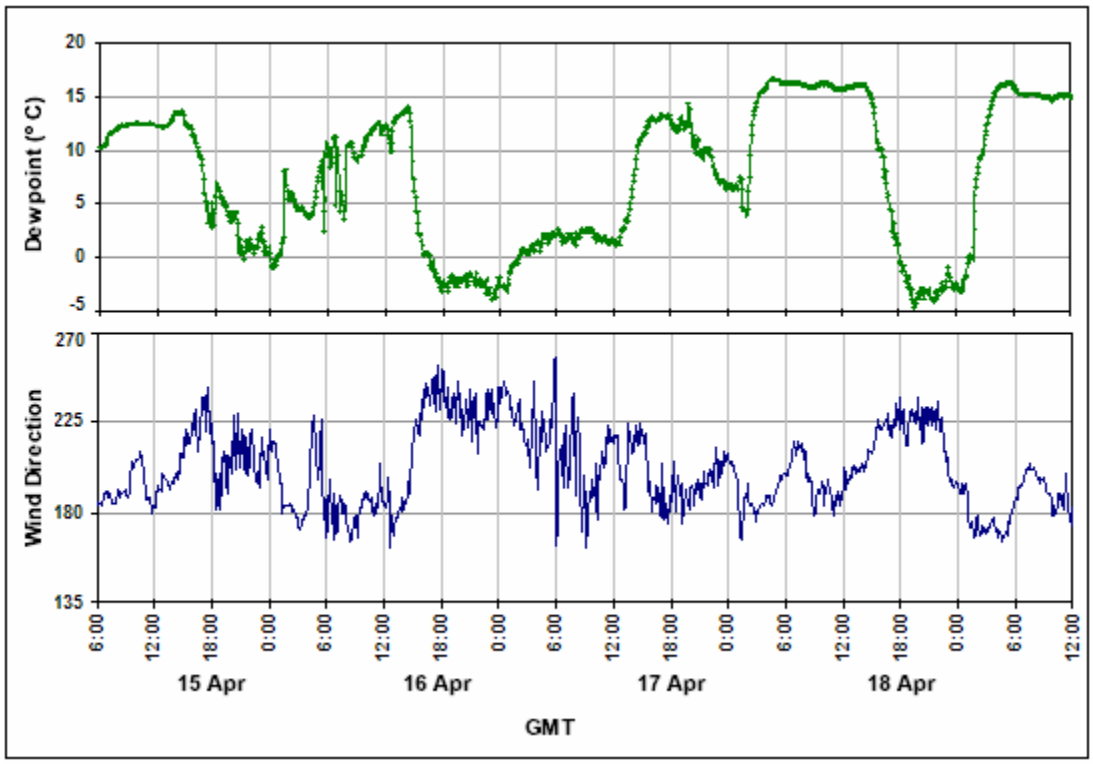

Figure 4. Time series plots of dewpoint temperature and wind direction from the West Texas Mesonet site at Reese Center – near the center of the domain. The four dryline oscillations can be seen in the trace. Note the approximate mirror-image appearance to the two graphs, with veering winds associated with decreasing dewpoint and vise versa.

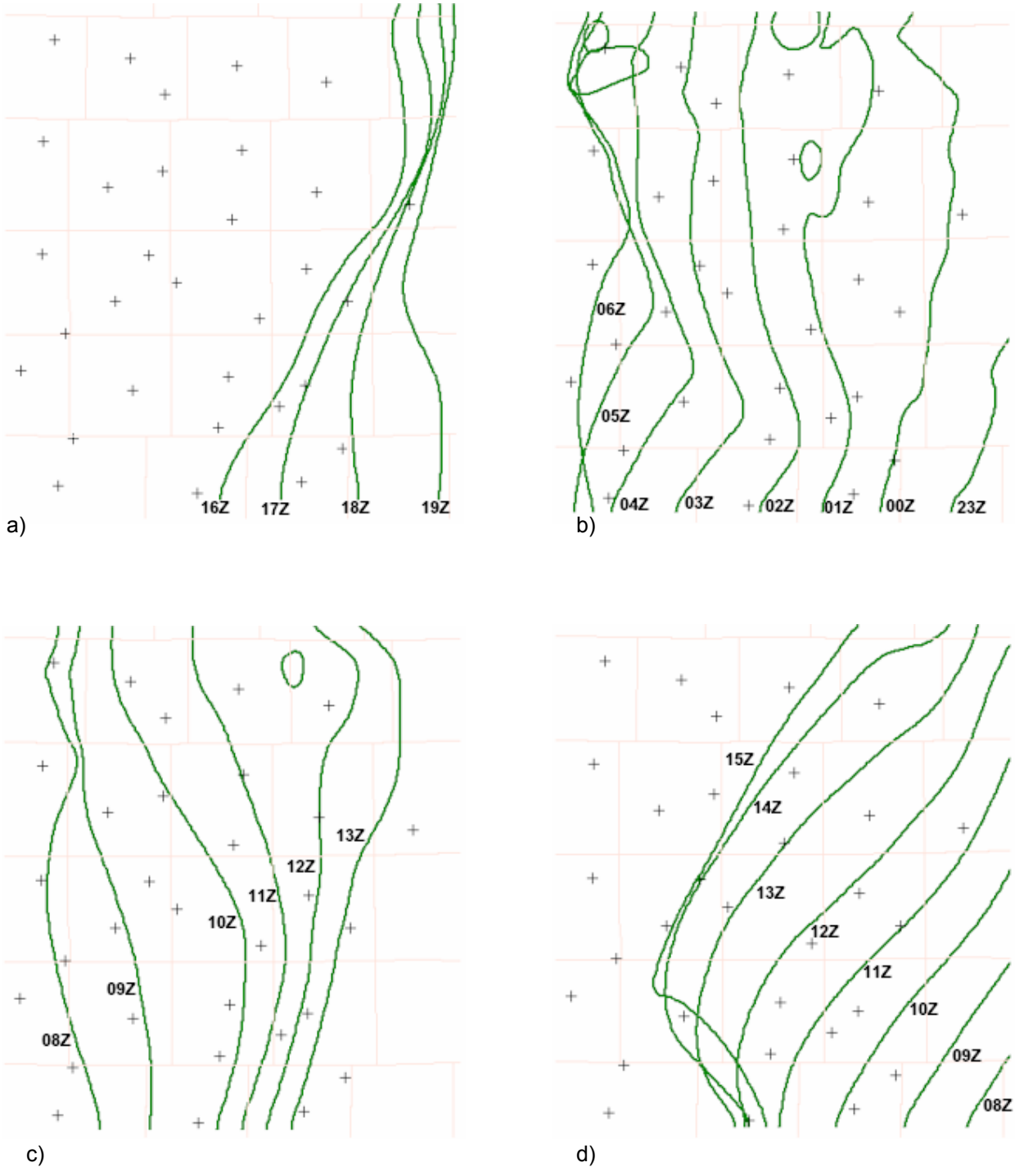

Figure 5. Plots of the 8.5 gkg^{-1} mixing ratio contour from the MM5 output for: a) 16 – 19 GMT 15 April, b). 23 – 06 GMT 15-16 April, c) 08 – 13 GMT 16 April, and d) 08 – 15 GMT 17 April.

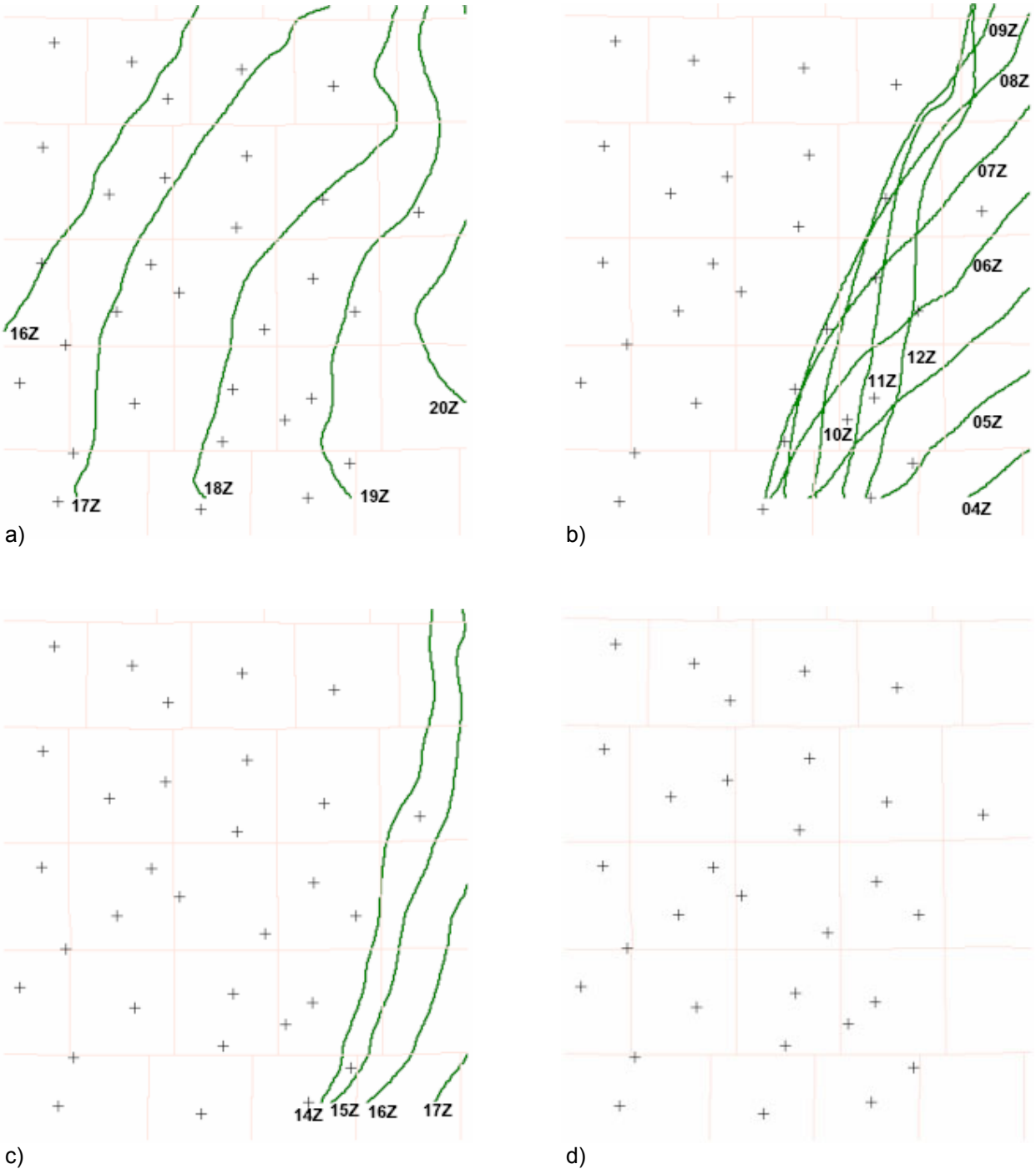

Figure 6. Plots of the 8.5 gkg^{-1} mixing ratio contour from the RAMS output for: a) 16 – 19 GMT 15 April, b). 04 – 11 GMT 16 April, c) 14 – 18 GMT 16 April, and d) 11 – 16Z 17 April.

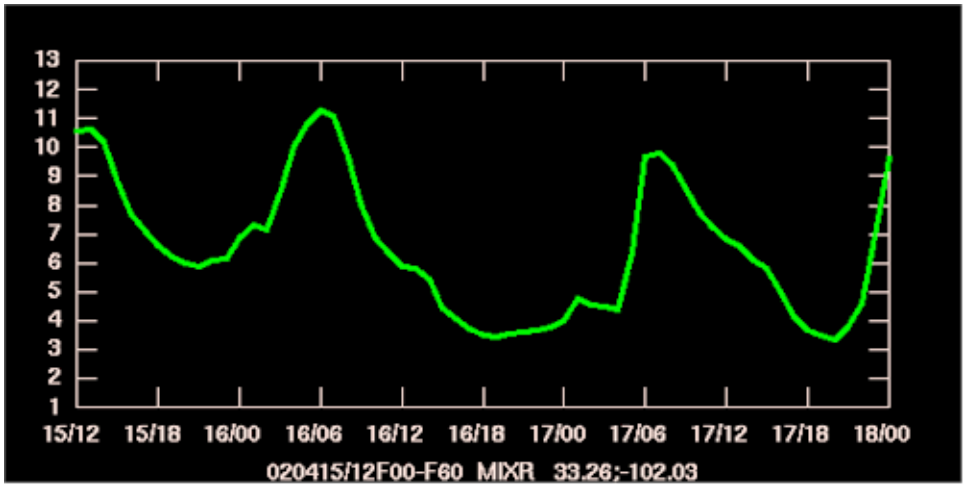

a)

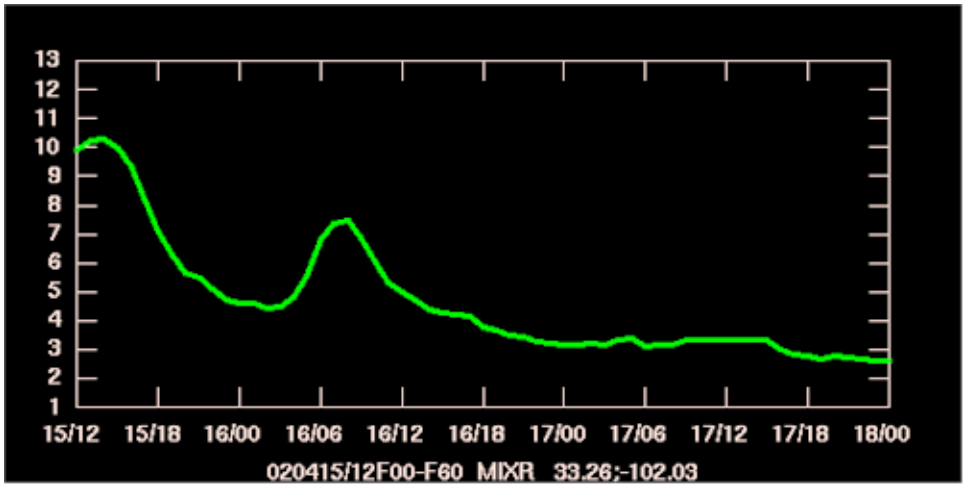

b)

Figure 7. Plots of the mixing ratio (gkg^{-1}) from the a) MM5 output, b) RAMS output, interpolated to the Reese Center Mesonet site (refer to figure 4 for comparison).

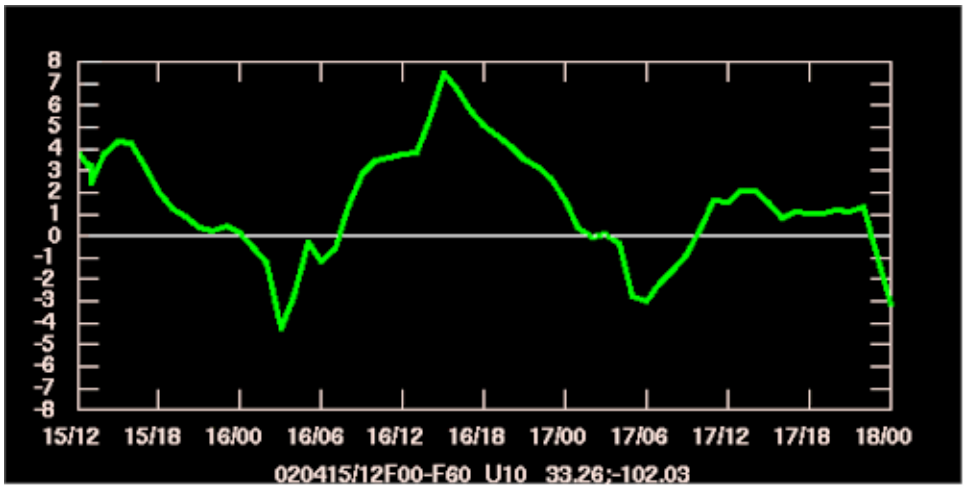

a)

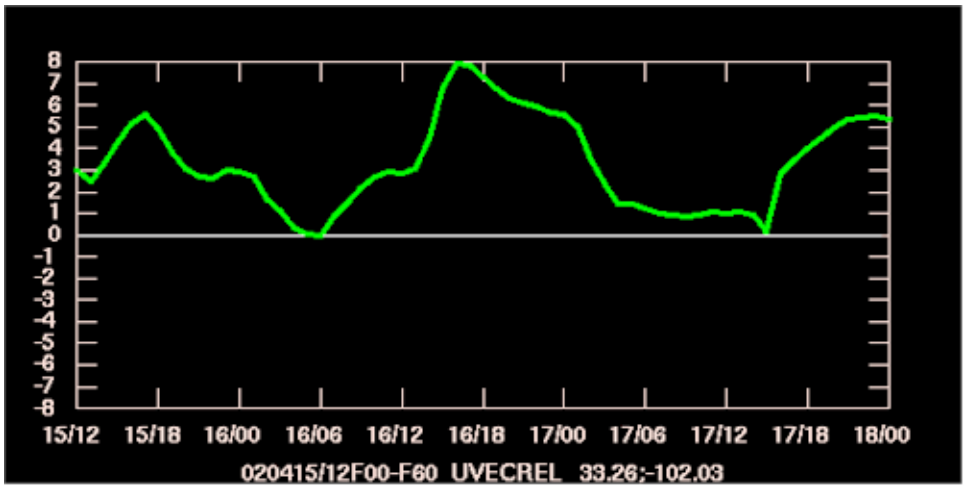

b)

Figure 8. Plots of the u-component of the surface wind (m s^{-1}) from the a) MM5 output, b) RAMS output, interpolated to the Reese Center Mesonet site (refer to figure 4 for comparison).